Insights into Space Solar Cell Durability Using SPICE Simulation Seeded by Current-Voltage Characteristics Parametrized Using the Lambert W Special Function

Timothy J Peshek *, Charity F.G. Sotero†, Emily N. Mathur‡, Calvin R. Robinson* and Herbert W. Schilling *
* John H. Glenn Research Center, The National Aeronautics and Space Administration, Cleveland, Ohio, 44135
Email: timothy.j.peshek@nasa.gov
†Department of Mathematics and Statistics, California State University at Long Beach, Long Beach, California, 90840.
‡Department of Mathematics, University of Southern California, Los Angeles, California, 90007.

***Abstract* — We developed and validated an automated routine for the fitting of I-V curve data to the single diode model according to an exact analytical solution. Our fitting routine was validated to show good noise immunity and high accuracy using simulated values from LTSPICE. We are thus able to automate parameter extraction from a dataset or arbitrary size. This parameterization allows for better simulation of performance of real cells and arrays and provides utility for a host of applications relevant to space arrays. We will use this methodology to determine the array performance of radiated cells over time, and simulate the performance of the arrays with ctive bypass diodes and power electronics.**

***Index Terms* — Space solar, bypass diodes, SPICE, I-V curves**

I. Introduction and Background

The single-diode model of solar cell behavior is an accepted model that well-mimics typical I-V curve behavior and provides a common language for researchers.[1], [2], [3] However, the model is limited in utility by the transcendental nature of the current as a function of voltage and cannot be solved explicitly without invoking special functions. [4], [5], [6] Numerous authors have proposed methodologies to solve this problem and develop models but many are fundamentally lacking because they involve assumptions or some human interaction. [7], [8], [9] Peshek et al. reviewed many of these techniques found that they all tended to suffer from fundamental issues, [10] summarized here as:

- The series and/or shunt resistances could not be estimated accurately without making assumptions that might not hold for degraded cells
- Series and shunt resistances and ideality factor could not be estimated accurately without a human selecting a fitting range, which negated potential automated processing
- Modeling of arrays of cells was highly error prone because of the lack of bypass diode inclusion and an inability to incorporate a distribution of parameters.

We describe here a potential solution to these issues using a generalized methodology that can be pipelined and used with an dataset of arbitrary size while solving the analytical single-diode model. Our solution utilizes a custom fitting routine and the Simulation Program with Integrated Circuit Emphasis, or "SPICE", which is a circuit modeling engine invoking a Newton-Raphson methodology for solving circuit node voltages and currents. Hence when an equivalent circuit model of a solar cell is encoded in SPICE it becomes a useful path to model solar cell behavior including I-V curves, quantum efficiency and even defects. [11] SPICE has been used to model solar cells and arrays in the past and applications from cell cracking and power losses, power electronics and even arc-faulting. [12], [13], [14], [15] The power of SPICE is that arrays of arbitrary size and construction can be simulated and bypass diodes included to predict performance under a host of conditions and evolution over time. The variables input into the simulations are seeded by the fitted output of a custom, and open-source project to develop an automated single-diode data-fitting routine based on the Lambert-W function.

In earlier work Peshek et al. noted that conventional equivalent circuit models of solar arrays, collections of interconnected cells, were often incomplete because the presence of bypass diodes were not necessarily included. [16] Indeed, in that work the authors motivated a concept that heterogeneity in performance that is observed upon degradation could manifest as bypass diode turn on, even under uniform irradiance, because of the current imbalance caused by a cell-level change in the local series or shunt resistance. Simulations using a version of SPICE by Linear Technology, or LTSPICE, showed that during bypass diode turn on, the turn on voltage would shift dependent upon the global distribution of cellular series resistance. Further, simulations in LTSPICE indicated that a discrepancy in series resistance among cells could lead to bypass diode turn on even under uniform irradiance, and this observation was proven experimentally. [10] Thus

the authors hypothesized that non-uniform degradation could be observed and the distribution of parameters in an array potentially quantified by locating the voltage and current of bypass turn on.

Support for the hypothesis has been provided by Hu et al. when analyzing a time series collection of 2.2 million I-V curves collected from engineered sites in three disparate locales. [17] Hu et al. found that the prevalence for bypass turn on increase steadily over time, after finding zero bypassing in the first two years of operation after installation. This increase in bypassing was commensurate with degradation curves, hence tracking bypassing can act as a proxy for degradation-induced power loss. [18]

II. Theory

To model the $I-V$ curve of an arbitrary solar cell a macroscopic physics-based model consisting of a current source, single *pn* diode, and two resistors is typically utilized [1]. Often, researchers may also add a parallel second diode, or "recombination diode" that describes an internal carrier recombination process that is nonlinear [19], [20].

Applying Kirchoff's laws and the Shockley equation yields the relationship between current (I) and voltage (V) for a solar cell in this single-diode model:

$$I(V,T) = I_L - I_0 \exp\left(\frac{V+IR_S}{N_s n V_{th}(T)} - 1\right) - \frac{V+IR_S}{R_{sh}}, \quad (1)$$

where I_L is the light induced current from photon absorption, I_0 is the reverse saturation current, N_s is the number of cells in the module, n is the diode ideality factor, R_s is the cell series resistance, R_{sh} is the cell shunt resistance, V_{th} is the thermal voltage equal to q/kT, where q is the elementary charge of an electron and k is Boltzmann's constant. Because of the transcendental nature of equation (1), it is not possible to solve in terms of I(V) explicitly, except by means of the Lambert W function [4].

Analytical solutions to the transcendental equation exist based upon the Lambert-W function, [4], [21] that Ghani et al. [22] used to estimate the series, shunt resistances and diode ideality factor. This analytical solution for $I(V,T)$ is given by:

$$I(V,T) = \frac{(I_L - I_0) - N_s V/R_{sh}}{1 + R_s/R_{sh}} - \frac{nV_{th}}{R_s} \times W[F(V,T)]. \quad (2)$$

Where $W[F(V,T)]$ is Lambert's W function, with $F(V,T)$, the functional, equaling:

$$F(V,T) = \frac{I_0\beta}{nV_{th}} \exp\left(\frac{N_s V}{nV_{th}}(1-\beta) + \frac{(I_L - I_0)\beta}{nV_{th}}\right) \quad (3)$$

where:

$$\beta = \frac{(R_s)}{(R_s + R_{sh})} \quad (4)$$

We utilized equation 2 to generate a fitting routine in 'R' that utilizes a combination of linear least-squares and Levenberg-Marquardt (LM) nonlinear fitting in an iterative manner in order to parametrize experimentally determined I-V curves and use the parameters in an LTSPICE simulation. This iterative, linear-least-squares-seeded LM method reduced sensitivity on initial guesses and allowed for nearly "blind" operation of the fitting. The algorithm utilized is shown as a flow chart in Figure 1.

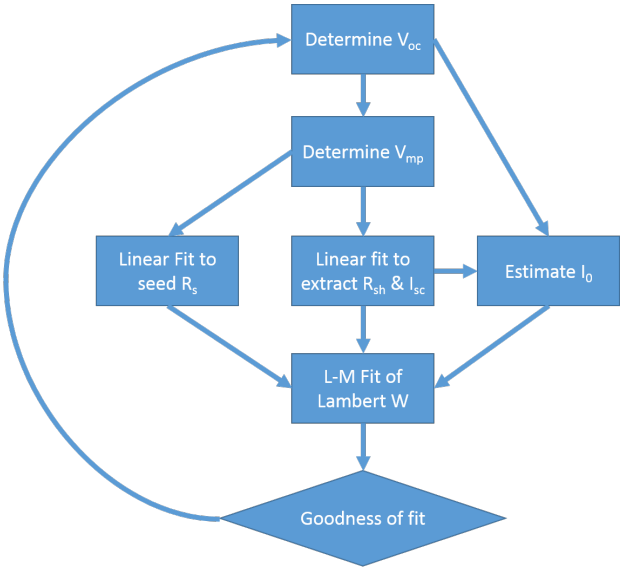

Fig. 1. flowchart

III. Validation Results

Our goal was to allow for arbitrary fitting of I-V curve data and yield a <1% error on the parameter extraction. For typical, well-behaved curves the goal was met easily for the diode-related parameters, that is the ideality factor, reverse saturation current and the light induced current.

In order to determine the relative effectiveness of the fitting routine we utilized several methods of validation. $I-V$ Curves were generated using the Lambert-W function analytical model with varying number of points and varying random noise and we found strong convergence and low errors on the predicted values. The fits would generally converge for data of only a few points, if those points included boundaries (I_{sc} and V_{oc}), midpoints (at least 2) between those boundaries and the maximum power point to help define the linear regions and enough points around the maximum power points (at least 7) to define the curvature.

We also found good resiliency to the influences of noise. Curves were generated for various numbers of points and an amount of random noise representative of a 1%, 2% or 5% measurement uncertainty in the current measurement was applied, as shown in Figure 2. Again, good convergence was found, where the predicted values agreed within uncertainty to the set values and the uncertainty in those predicted values scaled with the measurement uncertainty.

To understand further the utility of the model we determined the relative error of the model in extracting the series

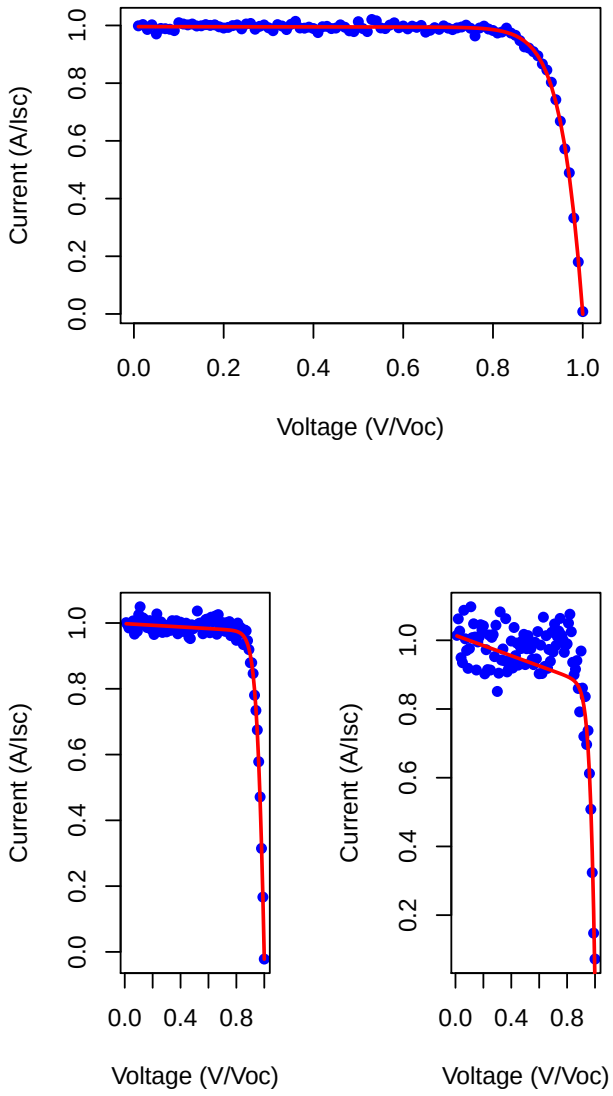

Fig. 2. I-V curves and prediction from fitting routine as a function of three different noise levels representing measurement uncertainty in the current values.

and shunt resistance values, R_s and R_{sh}, respectively. A series of $I-V$ curves were generated while allowing either R_s or R_{sh} to vary over a wide range and the relative error between the set value and the fitted value were computed. Qualitatively, As R_s becomes large and R_{sh} becomes small the % error increases very fast, *i.e.* as the $I-V$ curve becomes more linear. This response is reasonable because the data are more linear-like (even when generated by exponential functions) and can be modeled best by a line with two degrees of freedom and are over-fitted by models with five degrees of freedom (such as ours here). The overfitting leads to gross errors in all fitted values, but we will focus on the resistances.

The observation that fit error increases with degree of linearity suggests a valuable metric for determination of the model's boundaries. After fitting the single diode model to the dataset, we also fit a linear least squares curve and acquire the R^2 goodness of fit metric for determination of "linearity" of the $I-V$ curve. For example, a high fill factor (80%) curve will have a linear R^2 of about 0.2, and a fill factor less than 50% has a linear R^2 above 0.9 and is quickly approaching a line shape. The data for the % error in R_s and R_sh are shown for curves containing no noise in Figure 3.

The plots in Figure 3 show some interesting features. As expected the % error in the extracted values increases dramatically above linear $R^2 = 0.9$. Yet there are also unexpected behaviors in the R_s response: a small dip, fast rise towards a break, then a decay that mimics a hyperbolic function. The reason for this behavior appears to be in the fitting routine itself and the fact that the Lambert W-function has both real and imaginary branches and in this small regime the routine is actually trying to fit on the imaginary branch, which manifests as a computational "not a number" (NaN). For the R_{sh} we observe less dramatic behavior but it is interesting to note that the response of the % error function increases dramatically also for very low linear R^2, that is for very high fill factors. Hansen [6] explained this large error in R_{sh} is due to the difficulty in fitting a slope in this region where the $I-V$ response is flat, thus obtaining a very small number, and then inverting it to extract the shunt resistance, giving a very large number. This value is thus highly prone to errors and is extremely sensitive to noise in this regime. Yet, through this analysis we can provide a metric to understand and poredict the error in fitted values and provide boundaries and a methodology for fitting any abritrary dataset. A complete multidimensional contour plot would show the multidimensional boundaries to the fitting space, but is beyond the scope of this article.

IV. Case Study: Active Bypassing

As a potential application of this approach we will examine a simple circuit of active bypassing cells in a small array and determining the potential positive impact of such a configuration. In an active bypass circuit the typical silicon *pn* junction diode is used to drive a charge pump that can be used to turn on a logic-level field effect transistor to provide a much lower resistance bypass path. This alternate path can be used as a passive means of reducing the voltage drop across the bypass diode during current mismatch scenarios caused by damage or heterogeneous degradation as described in the introduction. We utilized a simple linear amplifier to drive the active bypass field effect transistor (FET), for simplicity in design, that had a very low quiescent current draw and during operation consumed approximately 0.5 mW at peak.

The solar arrays utilized were comprised of single diode cells with a silicon schottky bypass diode. The parameters were determined for this preliminary case study by fitting data from commercial datasheets, and the array was constructed

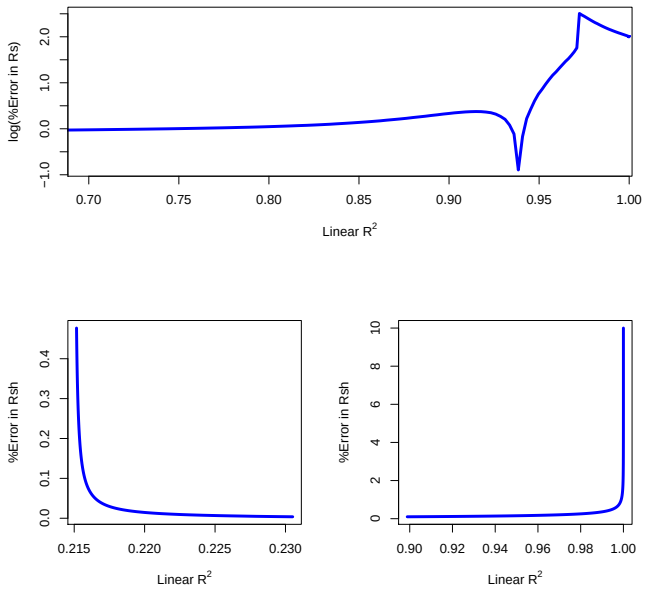

Fig. 3. A series of plots of the percent error in the determination of the series (top) and shunt (bottom left and right) resistances versus the R^2 goodness of fit measure of the data fitted using a linear function. Hence a very low R^2 is more like a typical $I-V$ curve with a high fill factor. An R^2 greater than 0.9 is very close to a line and represents a curve with a very low fill factor.

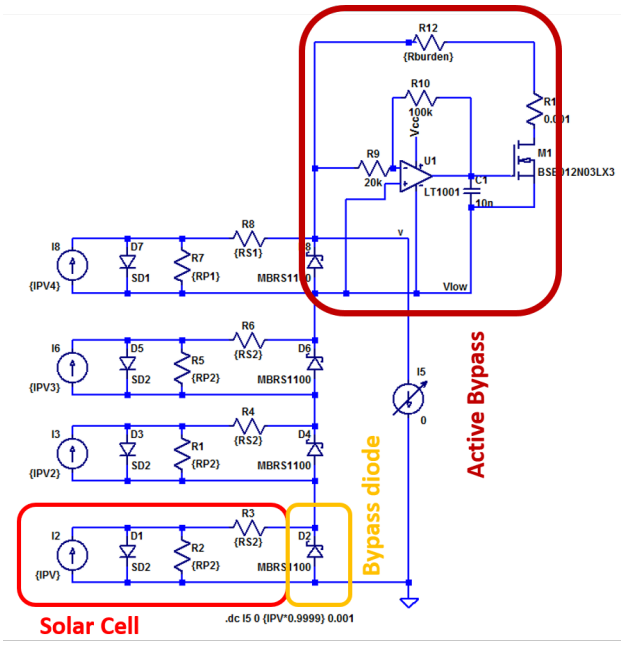

Fig. 4. A schematic of the circuit that was simulated in LTSPICE. The red box depicts the single diode model of a solar cell with schottky bypass diode called out in orange. Our active bypass circuitry, circled in dark red, was designed simply using a differential linear amplifier for simplicity and an external power supply, although a more robust and self contained design would include a charge pump and amplifier with gate driver to a logic level FET.

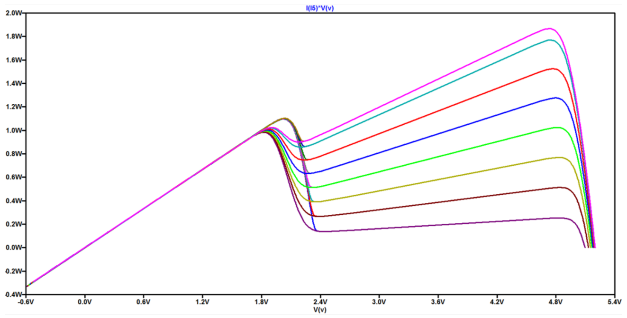

Fig. 5. The simulated $P-V$ curves with and without active bypassing as a function of 1 MeV electron fluence. Only the highest voltage cell is degraded with respect to the others and only that cell is modeled with an active bypass circuit.

to be 4 solar cells of equal beginning of life performance. The cell at the highest voltage in the array was then altered to mimic recently published data on performance of triple junction solar cells that had been exposed to high energy (1 MeV) electrons. [23] We allowed the short circuit current and reverse saturation current to vary in accordance with differing fluences of radiation and simulate performance over time. The cell responses in efficiency, fill factor, I_{sc} and V_{oc} were obtained from literature and using our fitting routine we were able to model the circuit parameters that can be utilized in a LTSPICE simulation. [23] Other cells were maintained as if they had incurred no damage in order to observe the effects of a worst-case heterogeneity.

Under the above scenario the difference in currents among the cells would cause the bypass diode to turn on under an I-V sweep of the array, and subsequently during this period the active bypass transistor also turned on. The simulations demonstrated a decrease in lost power during bypassing for the active circuit of 100 mW per bypass diode essentially irrespective of the current differential. Notably, the simulated I-V curves outside the region of bypassing showed no difference, suggesting that the gain in power may only occur under the specific conditions of the array being biased at or near the bypass turn on voltage. If maximum power point tracking (MPPT) power management system were used then the small gain in power would be utilized.

V. Conclusions

We have successfully developed a system for the automated parameterization of I-V curves according to the sigle diode model. Our goal is to use this fitting routine to seed and LTSPICE simulation of array performance with realistic values including a distribution of parameters. This methodology can then be used to determine the performance of cells over time. As a working case study we will use cells exposed to radiation to determine the distribution response function to 1 MeV electrons and model system performance to be presented at the conference. This effort is underway and using literature values to start the simulation we find that bypass diodes readily turn on for a radiation-exposed array. The simulations

then allow for testing of various mitigation schemes including where to bias the array, what performance is expected from a maximum power point tracking algorithm, and even lifetime performance modeling.

ACKNOWLEDGMENT

The authors are grateful to the NASA Glenn Research Center's Independent Research and Development Program for support of this work. Sotero and Mathur were funded under the NASA Higher Education Internship Program, contracted to the University Space Research Association, contract number NNX13AJ37A.

REFERENCES

[1] W. De Soto, S. A. Klein, and W. A. Beckman. Improvement and validation of a model for photovoltaic array performance. *Solar Energy*, 80(1):78–88, January 2006. 00465.

[2] Firoz Khan, S.N. Singh, and M. Husain. Effect of illumination intensity on cell parameters of a silicon solar cell. *Solar Energy Materials and Solar Cells*, 94(9):1473–1476, September 2010.

[3] T.J. McMahon, T.S. Basso, and S.R. Rummel. Cell shunt resistance and photovoltaic module performance. In , *Conference Record of the Twenty Fifth IEEE Photovoltaic Specialists Conference, 1996*, pages 1291–1294, 1996.

[4] Amit Jain and Avinashi Kapoor. Exact analytical solutions of the parameters of real solar cells using Lambert W-function. *Solar Energy Materials and Solar Cells*, 81(2):269–277, February 2004.

[5] F. Ghani, Mike Duke, and J. Carson. Numerical calculation of series and shunt resistance of a photovoltaic cell using the Lambert W-function: experimental evaluation. *Solar Energy*, 87:246–253, 2013.

[6] Clifford Hansen. Estimation of Parameters for Single Diode Models Using Measured IV Curves. In *39th IEEE Photovoltaic Specialists Conference, Tampa, FL*, 2013. 00002.

[7] D. Pysch, A. Mette, and S.W. Glunz. A review and comparison of different methods to determine the series resistance of solar cells. *Solar Energy Materials and Solar Cells*, 91(18):1698–1706, November 2007.

[8] Faisal GHANI, M. Duke, and J. Carson. Extraction of solar cell modelling parameters using the Lambert W function. In *Proceeding of the annual conference, Australian solar energy society, Melbourne*, 2012.

[9] Dezso Sera. Series resistance monitoring for photovoltaic modules in the vicinity of MPP. In *25th European Photovoltaic Solar Energy Conference and Exhibition*, pages 4506–4510, 2010.

[10] Timothy J. Peshek, Justin S. Fada, Yang Hu, Yifan Xu, Mohamed A. Elsaeiti, Erdmut Schnabel, Michael Köhl, and Roger H. French. Insights into metastability of photovoltaic materials at the mesoscale through massive I–V analytics. *Journal of Vacuum Science & Technology B, Nanotechnology and Microelectronics: Materials, Processing, Measurement, and Phenomena*, 34(5):050801, 2016.

[11] Luis Castañer and Santiago Silvestre. Modelling Photovoltaic Systems Using PSpice®. In *Modelling Photovoltaic Systems Using PSpice®*, pages i–xvii. John Wiley & Sons, Ltd, 2002.

[12] A. Zekry and A.Y. Al-Mazroo. A distributed SPICE-model of a solar cell. *IEEE Transactions on Electron Devices*, 43(5):691–700, 1996.

[13] Stefan Eidelloth, Felix Haase, and Rolf Brendel. Simulation Tool for Equivalent Circuit Modeling of Photovoltaic Devices. *IEEE Journal of Photovoltaics*, 2(4):572–579, October 2012.

[14] M Kontges, I Kunze, S Kajari-Schroder, X Breitenmoser, and B Bjorneklett. Origin and consequences of (micro)-cracks in crystalline silicon solar modules. *National Renewable Energy Laboratory, Colorado, USA*, 2011.

[15] Jack Flicker and Jay Johnson. Electrical simulations of series and parallel pv arc-faults. In *Photovoltaic Specialists Conference (PVSC), 2013 IEEE 39th*, pages 3165–3172. IEEE, 2013.

[16] Timothy J. Peshek, Shay Mathews, Yang Hu, and Roger H. French. Mirror augmented photovoltaics and time series analytics of the I–V curve parameters. In *Photovoltaic Specialist Conference (PVSC), 2014 IEEE 40th*, pages 2027–2031. IEEE, 2014.

[17] Yang Hu, Erdmut Schnabel, Michael Kohl, Roger H French, and Timothy J Peshek. Detecting heterogeneity in pv modules from massive real-world step iv curves: A machine learning approach. In *Photovoltaic Specialists Conference (PVSC), 2016 IEEE 43rd*, pages 0279–0285. IEEE, 2016.

[18] Yang Hu, Venkat Yashwanth Gunapati, Pei Zhao, Devin Gordon, Nicholas R Wheeler, Mohammad A Hossain, Timothy J Peshek, Laura S Bruckman, Guo-Qiang Zhang, and Roger H French. A nonrelational data warehouse for the analysis of field and laboratory data from multiple heterogeneous photovoltaic test sites. *IEEE Journal of Photovoltaics*, 7(1):230–236, 2017.

[19] A Hovinen. Fitting of the solar cell *IV* -curve to the two diode model. *Physica Scripta*, T54:175–176, January 1994. 00000.

[20] Z. Salam, K. Ishaque, and H. Taheri. An improved two-diode photovoltaic (PV) model for PV system. In *2010 Joint International Conference on Power Electronics, Drives and Energy Systems (PEDES) 2010 Power India*, pages 1–5, 2010.

[21] Amit Jain, Sandeep Sharma, and Avinashi Kapoor. Solar cell array parameters using Lambert W-function. *Solar Energy Materials and Solar Cells*, 90(1):25–31, 2006.

[22] F. Ghani, M. Duke, and J. Carson. Numerical calculation of series and shunt resistances and diode quality factor of a photovoltaic cell using the Lambert W-function. *Solar Energy*, 91:422–431, May 2013. 00006.

[23] Mitsuru Imaizumi, Tetsuya Nakamura, Tatsuya Takamoto, Takeshi Ohshima, and Michio Tajima. Radiation degradation characteristics of component subcells in inverted metamorphic triple-junction solar cells irradiated with electrons and protons. *Progress in Photovoltaics: Research and Applications*, 25(2):161–174, February 2017.